ACS APPLIED MATERIALS & INTERFACES

Research Article

www.acsami.org

Supramolecular Immobilization of Xanthine Oxidase on Electropolymerized Matrix of Functionalized Hybrid Gold Nanoparticles/Single-Walled Carbon Nanotubes for the Preparation of Electrochemical Biosensors

Reynaldo Villalonga,*[,†,‡] Paula Díez,[†] Marcos Eguílaz,[†] Paloma Martínez,[§] and José M. Pingarrón[†,‡,*]

[†]Department of Analytical Chemistry and [§]Department of Organic Chemistry I, Faculty of Chemistry, Complutense University of Madrid, 28040-Madrid, Spain

[‡]IMDEA Nanoscience, Cantoblanco University City, 28049-Madrid, Spain

Supporting Information

ABSTRACT: Glassy carbon electrodes modified with single-walled carbon nanotubes and a three-dimensional network of electropolymerized Au nanoparticles capped with 2-mercaptoethanesulfonic acid, *p*-aminothiophenol, and 1-adamantanethiol were used as hybrid electrochemical platforms for supramolecular immobilization of a synthesized artificial neoglycoenzyme of xanthine oxidase and β-cyclodextrin through host−guest interactions. The ensemble was further employed for the bioelectrochemical determination of xanthine. The biosensor showed fast amperometric response within 5 s and a linear behavior in the 50 nM to 9.5 μM xanthine concentration range with high sensitivity, 2.47 A/(M cm^2), and very low detection limit of 40 nM. The stability of the biosensor was significantly improved and the interferences caused by ascorbic and uric acids were noticeably minimized by coating the electrode surface with a Nafion thin film.

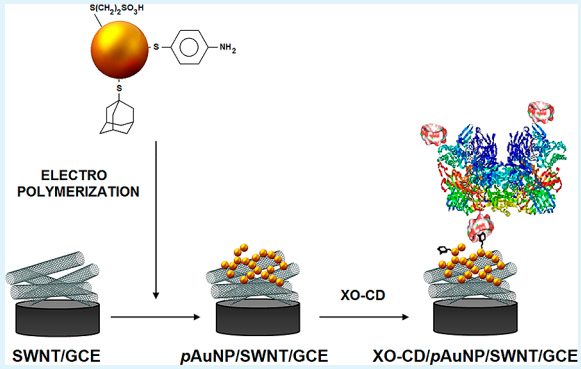

KEYWORDS: *single-walled carbon nanotube, gold nanoparticle, supramolecular assembly, enzyme biosensor, cyclodextrin*

INTRODUCTION

Electrochemical biosensors constitute one of the most rapidly evolving fields in chemistry. From an analytical point of view, they allow the design of portable and affordable sensing devices exhibiting high sensitivity and the characteristic specificity provided by biological recognition systems.[1,2] The successful development of this technology is linked to the rational design of novel electrode surfaces able to improve the speed of the electrochemical processes associated with the analytical responses as well as the stable immobilization of the biomolecules preserving their three-dimensional active conformation. In this context, electroconductive nanosized materials have been exhaustively employed to prepare novel nanostructured surfaces with improved performance.[3−7] This success relies on the unique properties of nanomaterials such as high surface energy and surface-to-volume ratio, ability to decrease proteins-nanomaterial distance, thermal stability, easy functionalization and the possibility to act as electroconductive wires between the electrodes and the redox centers in some biomolecules.[8] In particular, gold nanoparticles (AuNPs) and carbon nanotubes (CNTs) have been at the central core of novel advanced materials widely used in biosensor technology.[6,8−11] Furthermore, the combination of these nanomaterials to prepare synergic hybrid nanomaterials has demonstrated to constitute a successful strategy to construct electrochemical interfaces with unique properties for the preparation of more efficient and robust biosensors.[12]

The synthesis of novel polyfunctionalized gold nanoparticles, bearing aniline moieties able to be electropolymerized to form electroconductive three-dimensional networks on electrodes, as well as their use for the preparation of molecularly imprinted surfaces suitable for the construction of SPR biosensors, has been recently reported.[13,14] Furthermore, our group demonstrated recently the usefulness of such electropolymerized nanostructures for the construction of enzyme electrochemical biosensors. In this context, the preparation of metal surfaces nanostructured with networks of Au nanoparticles functionalized with boronic acid and PAMAM dendron moieties to design amperometric biosensors toward hydrogen peroxide and cathecol, respectively, were reported.[15,16] However, to the best of our knowledge, the combined use of these electro-

Received: June 1, 2012
Accepted: July 16, 2012
Published: July 16, 2012

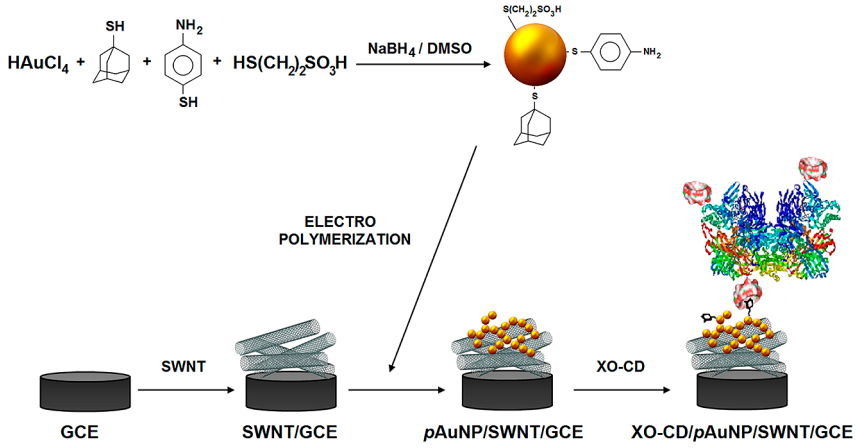

Figure 1. Schematic display of the steps involved in the preparation of XO-CD/*p*AuNP/SWNT/GCE enzyme biosensors.

polymerized nanoparticle networks with other nanomaterials has not been evaluated until now.

On the other hand, the use of host−guest supramolecular interactions was previously proposed as a soft, reversible and multivalence method for the immobilization of enzymes on metal nanoparticles and surfaces taking advantage of the complementary interaction of adamantane derivatives with *β*-cyclodextrin (CD).[17−19] This strategy was successfully employed to construct stable enzyme biosensors.[20−22]

This work describes a novel approach for the construction of a nanostructured electrode surface by electropolymerization of polyfunctionalized Au nanoparticles on a glassy carbon electrode (GCE) which was previously coated with single-walled carbon nanotubes (SWNT). For this purpose, Au nanoparticles modified with 2-mercaptoethanesulfonic acid, 1-adamantanethiol, and *p*-aminothiophenol were synthesized and further electropolymerized on the SWNT-coated GCE through the formation of a bisaniline-cross-linked network. The presence of pendant adamantane residues in this electroconductive matrix allows the subsequent supramolecular immobilization of CD-based neoglycoproteins by formation of the complementary host−guest inclusion complexes. As a model system to demonstrate this proof of concept, we prepared a CD-modified xanthine oxidase (XO, EC 1.17.3.2) derivative which was employed as the target neoglycoprotein. Moreover, an electrochemical enzyme biosensor for xanthine based on this supramolecular design was constructed and evaluated.

2. MATERIALS AND METHODS

2.1. Reagents. Xanthine oxidase (Type III, 1.3 U/mg), $HAuCl_4$, $NaBH_4$, 2-mercaptoethanesulfonic acid, *p*-aminothiophenol, 1-adamantanethiol, and CD were purchased from Sigma-Aldrich Co. (USA). SWNT were from Wako Pure Chemical Industries, Ltd. (Japan). All other chemicals were of analytical grade.

2.2. Apparatus and Electrodes. Electrochemical impedance spectroscopy and cyclic voltammetry were performed using a FRA2 *μ*Autolab Type III potentiostat/galvanostat and data were acquired using Frequency Response Analyzer and GPES Ver. 4.9 software, respectively (Metrohm Autolab B.V., The Netherlands). Amperometric measurements were carried out with a dual-channel ultrasensitive InBea potentiostat (InBea Biosensores S.L., Spain). A conventional three-electrode system was employed for all electrochemical measurements. The working electrode was a glassy carbon electrode (GCE, 3.0 mm diameter) coated with SWNT, the electropolymerized network of Au nanoparticles and the immobilized CD-enzyme derivative (XO-CD/*p*AuNP/SWNT/GCE). This electrode coated with a Nafion thin film (Naf/XO-CD/*p*AuNP/SWNT/GCE) was evaluated for biosensing xanthine. An Ag/AgCl/KCl (3 M) and a Pt wire were used as reference and counter electrodes, respectively.

High resolution transmission electron microscopy (HR-TEM) measurements were performed with a JEOL JEM-3000 F microscope. The surface morphology of the electrode surface was characterized using high resolution field emission scanning electron microscopy (FE-SEM) with a JEOL JSM-6335F electron microscope (JEOL Ltd., Japan). FT-IR spectra were acquired with a Perkin-Elmer instrument. Spectrophotometric measurements were performed using an Agilent 8453 UV/vis spectrophotometer (Hewlett-Packard, USA).

2.3. Electrochemical Measurements. All measurements with the prepared bioelectrodes were carried out at 25 °C in 0.1 M sodium phosphate buffer, pH 7.0 (working volume 10 mL). The solution was stirred at 300 rpm with a magnetic bar during amperometric measurements, and 100 *μ*M xanthine solutions in 50 mM sodium phosphate buffer, pH 7.0, were freshly prepared.

2.4. Preparation of Nanomaterials. To prepare the adamantane-caped Au nanoparticles, we dissolved 197 mg of $HAuCl_4$ in 50 mL of deaerated DMSO. This solution was added dropwise to 50 mL of deaerated DMSO containing 284 mg of $NaBH_4$, 36 mg of 2-mercaptoethanesulfonic acid, 11 mg of 1-adamantanethiol, and 8 mg of *p*-aminothiophenol under vigorous stirring. The reaction mixture turned deep brown immediately, but the reaction was allowed to proceed for 24 h. The polyfunctionalized nanoparticles prepared in this way were precipitated by adding 50 mL CH_3CN, collected by centrifugation and washed with 50 mL of CH_3CN:DMSO (1:1 v/v), 50 mL of ethanol, and 50 mL of diethyl ether. The nanoparticles were finally isolated by centrifugation and dried under N_2.

SWNT were purified and partially oxidized by treatment with a mixture of HNO_3/H_2SO_4 (3:1, v/v) during 2 h in an ultrasonic bath. The treated nanotubes were centrifuged, washed with double distilled water until neutral pH, and finally dried in vacuum under P_2O_5.

These nanomaterials were characterized by FT-IR and HR-TEM.

2.5. Preparation of the Enzyme Electrode. The mono-6-ethylenediamino-6-deoxy-*β*-cyclodextrin was obtained by treating the corresponding mono-6-*O*-tosyl derivative[23] with freshly distilled ethylenediamine as reported previously.[24] XO was covalently glycosylated with this CD derivative via a carbodiimide-catalyzed reaction (XO-CD) as previously described.[22] The modified enzyme contained an average of 12 mol of CD residues attached to each mol of protein, as determined by the phenol-sulfuric acid assay.

To prepare the enzyme-modified electrode, a we polished bare GCE to mirrorlike surface with alumina powder (0.3 *μ*m), rinsed thoroughly with double distilled water, successively washed with double distilled water, anhydrous ethanol, and acetone in an ultrasonic bath, and dried under N_2 before use.

Coating of the treated GCE was accomplished by depositing two 10 *μ*L aliquots of a 0.4 mg/mL aqueous dispersion of SWNT on the

electrode surface and allowing drying. The SWNT-modified electrode was then dipped into a 2 mg/mL Au nanoparticles solution in 0.1 M H_2SO_4 and electropolymerization was accomplished by cycling the potential 10 times between −0.35 and +0.85 V vs Ag/AgCl at a scan rate of 100 mV/s, followed by applying a constant potential of 0.85 V for 1 h. The electrode modified with the electropolymerized bisaniline-cross-linked network of Au nanoparticles (*p*AuNP/SWNT/GCE) was exhaustively washed with 0.1 M H_2SO_4 and double distilled water before enzyme immobilization.

Subsequently, the *p*AuNP/SWNT/GCE was dipped into a 5 mg/mL XO-CD solution in 50 mM sodium phosphate buffer, pH 7.0, for 4 h. The enzyme-modified electrode (XO-CD/*p*AuNP/SWNT/GCE) was finally washed with the same cool buffer, dried under nitrogen and kept at 4 °C until use. A Nafion thin film-coated enzyme electrode (Naf/XO-CD/*p*AuNP/SWNT/GCE) was also prepared by dropping 5.0 μL of a 0.5% (v/v) Nafion ethanolic solution on the surface of the XO-CD/*p*AuNP/SWNT/GCE and dried, washed, and stored as described above.

3. RESULTS AND DISCUSSION

3.1. Preparation and Characterization of the Nanostructured Bioelectrode. The steps involved in the preparation of the hybrid nanostructured enzyme electrode are schematized in Figure 1. Polyfunctionalyzed AuNPs were first synthesized by reducing $AuCl_4^-$ ions with $NaBH_4$ in a DMSO solution containing 1-adamantanethiol, 2-mercaptoethanesulfonic acid and *p*-aminothiophenol in a 1.3:3.4:1 molar ratio. Dark red and water-soluble nanoparticles were obtained by applying this procedure.

HR-TEM analysis of the obtained nanoparticles showed spherical geometry with an average diameter of 4.9 ± 0.8 nm (see the Supporting Information), which is similar to the size reported for other polyfunctionalized Au nanoparticles bearing other capping ligands.[15,16,19]

Figure 2 shows an FT-IR spectrum of the polyfunctionalyzed nanoparticles. The presence of aniline residues in the

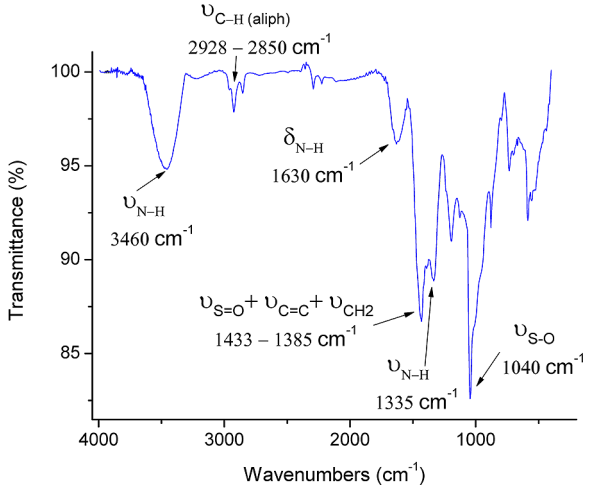

Figure 2. FT-IR spectrum of the polyfunctionalized Au nanoparticles.

nanomaterial was revealed by the broad and intense band around 3460 cm^{-1}, corresponding to the stretch vibration of the N−H bonds. In addition, the presence of aniline moieties was confirmed by the bands at 1630 and 1335 cm^{-1}, corresponding to the N−H blending and C−N stretching, respectively. This latter band is partially overlapped with the large band appearing in the range of 1433 to 1385 cm^{-1}, which can be ascribed to the overlapped S═O and C═C stretching vibrations and CH_2 blending, suggesting the presence of sulfonate, aromatic and aliphatic groups in the modified nanoparticles, respectively. The presence of sufonate residues can be also supported by the intense stretching vibration band of the S−O bonds at 1040 cm^{-1}, as well as by the stretching of aliphatic C−H bonds at 2850 cm^{-1}. On the other hand, adamantane residues were confirmed by the C−H stretching vibration at 2928 cm^{-1} revealing the presence of a cyclic aliphatic compound on the nanoparticles surface. Finally, the formation of a covalent Au−S bond is supported by the presence of the large band in the range of 500 to 750 cm^{-1} that can be assigned to stretch the mode of C−S groups.[25]

It should be highlighted that the employed synthetic approach ensured the preparation of Au nanoparticles with the appropriate characteristics allowing their use as structural units for the electrochemical formation of the nanostructured three-dimensional matrix. In fact, the growing of the metal colloid in the mixture containing the thiol derivatives provided the formation of small and spherical capped nanoparticles. Furthermore, it should be mentioned that the used thiol derivatives were specifically selected to confer some relevant properties to the synthesized Au nanoparticles: solubility (2-mercaptoethanesulfonic acid), polimerization ability (*p*-aminothiophenol) and capability to form inclusion complexes with CDs (1-adamantanethiol).

The formation of host−guest complexes on the Au nanoparticle surface with the CD-modified xanthine oxidase derivative was confirmed by UV/vis spectrophotometry. Figure 3 shows the spectra of the polyfunctionalized AuNPs dissolved

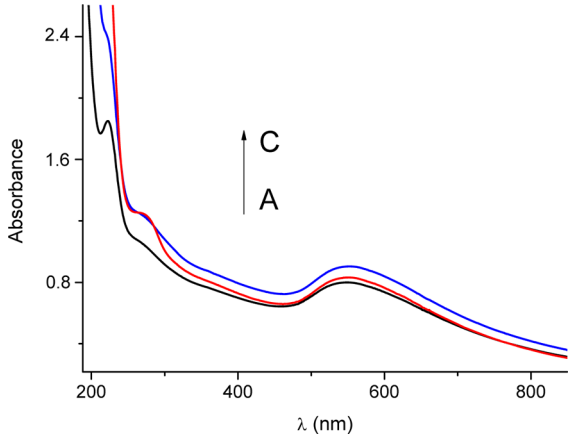

Figure 3. UV−vis spectra of 0.4 mg/mL solution of Au nanoparticles in 50 mM sodium phosphate buffer, pH 7.0 (A) without and (B, C) with (B) 0.5 mg/mL XO and (C) XO-CD.

in 50 mM sodium phosphate buffer pH 7.0 where the occurrence of a plasmon resonance absorption band with a maximum around 550 nm can be observed. The intensity of this band was slightly affected after addition of native XO, probably due to the electrostatic interaction of the enzyme with the nanoparticles surface. However, the intensity of the plasmon resonance band exhibited a significant increase when XO-CD was added to the nanoparticle solution and the maximum slightly shifted to around 552 nm. This effect could be related to the association of the modified enzyme to the metal nanoparticles surface through the formation of inclusion complexes between the complementary adamantane and CD residues. Similar plasmonic effects were previously reported for

CD-coated Au nanoparticles after association with adamantane-modified enzymes.[19]

Polyfunctionalized Au nanoparticles were electropolymerized on the surface of SWNT-coated GCE through two sequential steps.[13−16] These steps involved first the formation of a bisaniline-cross-linked network of nanoparticles by performing cyclic voltammetric scans between −0.35 V and +0.85 V in 0.1 M H_2SO_4, and a further growing of the Au nanoparticle-based polymer for 1 h at a constant potential of +0.85 V. Figure 4

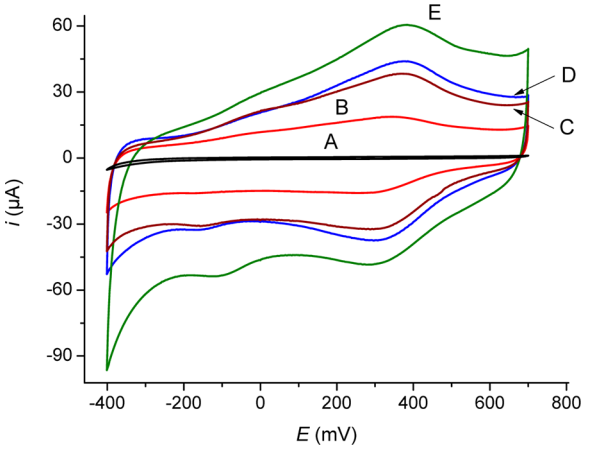

Figure 4. Cyclic voltammograms recorded in 0.1 M H_2SO_4 at (A) a bare GCE, (B) a SWNT-modified GCE, upon electropolymerization of Au nanoparticles for (C) five and (D) ten potential cycles, and (E) after polymer growing for 1 h at +850 mV. Scan rate: 50 mV/s.

shows the cyclic voltammograms recorded in 0.1 M H_2SO_4 solution upon the different electrode modification steps. As expected, a remarkable larger background current was observed at the SWNT-modified electrode in comparison with the bare GCE, which can be attributed to the much larger active surface area of nanotubes electrically connected to the electrode surface.[26] The repeated potential scanning in the Au nanoparticle solution produced a noticeable increase in the background current as a consequence of the increase in the electrochemical surface area caused by the generation of the electropolymerized network of metal nanoparticles on the electrode surface.

In addition, the appearance of an anodic peak at +0.380 V and two cathodic peaks around +0.300 V and −0.130 V was observed. The current intensity of these peaks increased when the number of cycles increased, indicating the electrochemical formation of bis-aniline condensation adducts.[27] The current intensity of these peaks, as well as the background current in the cyclic voltammogram were larger after the second step of electropolymerization performed during one hour at a fixed potential of +0.85 V (voltammogram E), indicating the growing of a dense three-dimensional electroconductive assembly of Au nanoparticles on the electrode surface via bis-aniline linkages.

Figure 5 shows the FE-SEM image of the electrode surface after the electropolymerization processes. A three-dimensional nanostructured network of small and spherical Au nanoparticles covering the SWNT-coated surface can be observed. It should be noted that the electropolymerized matrix was composed of a nonordered array of AuNPs-based protuberances of different heights, separated by irregularly distributed nanoholes on the SWNT-coated GCE surface. This topology ensures a high

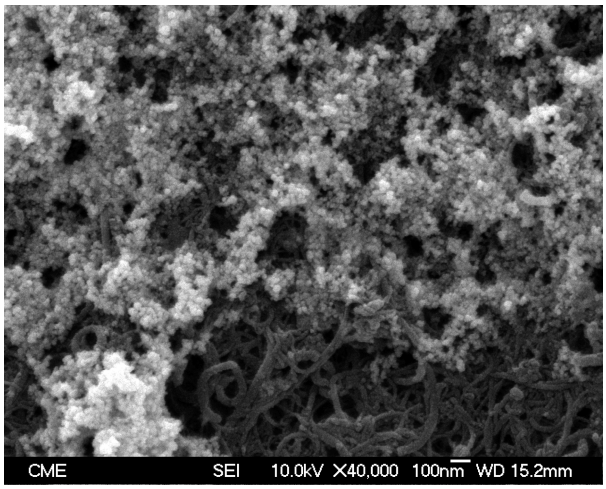

Figure 5. Field-emission SEM image of the *p*AuNP/SWNT/GCE.

functionalized metal surface area on the electrode to favor the further immobilization of the enzyme derivative.

To evaluate the potential bioanalytical use of this novel nanostructured electrode surface, we employed a XO-CD neoglycoenzyme as a probe of concept for constructing a biosensor device toward xanthine. Electrochemical impedance spectroscopy was performed in a 5 mM $[Fe(CN)_6]^{4-/3-}$ solution in 0.1 M KCl to evaluate the interfacial changes occurring during the different functionalization steps. As it can be seen in Figure 6, a noticeable decrease in the semicircle

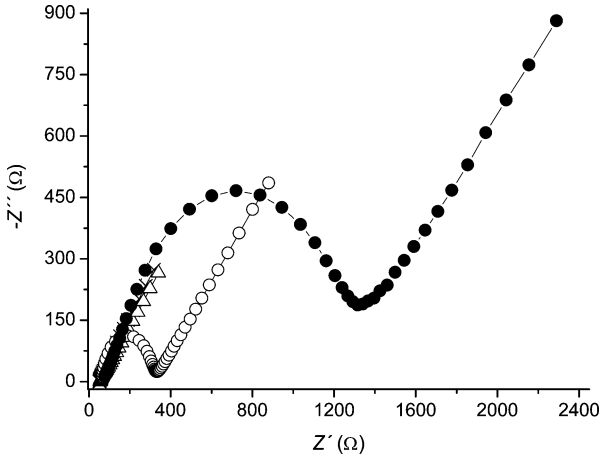

Figure 6. Nyquist plots of bare GCE (○), SWNT/GCE (Δ), *p*AuNP/SWNT/GCE (X), and XO-CD/*p*AuNP/SWNT/GCE (●) in 0.1 M KCl solution containing 5 mM $K_3[Fe(CN)_6]/K_4[Fe(CN)_6]$ (1:1).

diameter of the Nyquist plot occurred after modification of the bare GCE with SWNTs and the subsequent electropolymerization of Au nanoparticles, indicating the expected increase in the electron transfer rate between the redox probe and the nanostructured electrode surface. However, immobilization of XO-CD caused a significant insulating effect on the electrode surface with a remarkable increase in the R_{et} value for the enzyme-modified electrode.

This effect suggested a high enzyme loading on the electrode surface which is a desired attribute for biosensing purposes. These results were confirmed by cyclic voltammentry in the same working solution for the different electrode architectures (Figure 7). Bare, SWNT, and Au nanoparticle-modified GCE

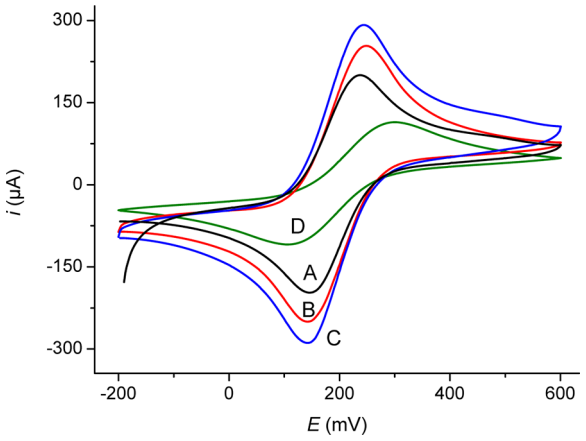

Figure 7. Cyclic voltammograms recorded in 0.1 M KCl solution containing 5 mM $K_3[Fe(CN)_6]/K_4[Fe(CN)_6]$ (1:1) at (A) bare GCE, (B) SWNT/GCE, (C) *p*AuNP/SWNT/GCE, and (D) XO-CD/*p*AuNP/SWNT/GCE. Scan rate: 50 mV/s.

showed well-defined typical quasi-reversible diffusion-limited patterns with ΔE values of 90, 103, and 101 mV and i_a/i_c ratios of 0.99, 1.03, and 1.01, respectively. Moreover, coating with SWNT and further electropolymerization of the metal nanoparticles increased the electrochemical surface area of the GCE, as revealed by the higher peak currents obtained. By using the Randles-Sevcik model, the electrochemical surface area of the GCE was estimated to increase from 7.1 to 9.7 and 11.1 mm^2 after sequential modification with SWNT and electropolymerized Au nanoparticles, respectively. This fact can be justified by the electroconductive nature of both the SWNT and the bisaniline cross-linked Au nanoparticle-based matrix.

Conversely, a larger separation between the anodic and cathodic peaks, ΔE = 188 mV, and a noticeable decrease in the peak currents with i_a/i_c = 0.93 was produced after the modified electrode incubation in the XO-CD solution, indicating that the immobilized enzyme behaved as a kinetic barrier. A noticeable reduction to 3.9 mm^2 for the electroactive surface area was also observed at the enzyme-modified electrode, suggesting a high surface coverage with the XO-CD derivative in agreement with the results obtained by electrochemical impedance spectroscopy.

Figure 8A displays the cyclic voltammograms recorded at *p*AuNP/SWNT/GCE functionalized with native (curve b) and CD-modified XO (curve a) in 0.1 M sodium phosphate buffer, pH 7.0, aerated solutions at a scan rate of 50 mV/s. The anodic current significantly increased at both modified electrodes after addition of 200 μM xanthine, showing a peak current at +0.69 V corresponding to the enzymatic transformation of xanthine at the electrode surfaces and the further oxidation of the produced H_2O_2. However, the anodic peak current was 1.7-fold higher at the XO-CD/*p*AuNP/SWNT/GCE (curve d) in comparison with that recorded at the electrode modified with native XO (curve c), suggesting a higher active enzyme loading on the former bioelectrode. This fact should be related to the occurrence of host−guest interactions between the adamantane units at the AuNPs surface and the CD moieties attached to the enzyme.

The contribution of these supramolecular interactions to the overall immobilization process for XO-CD on *p*AuNP/SWNT/GCE was evaluated by recording a cyclic voltammogram in a 200 μM xanthine solution after one hour incubation of the enzyme electrode at 4 °C in 0.1 M sodium phosphate buffer pH

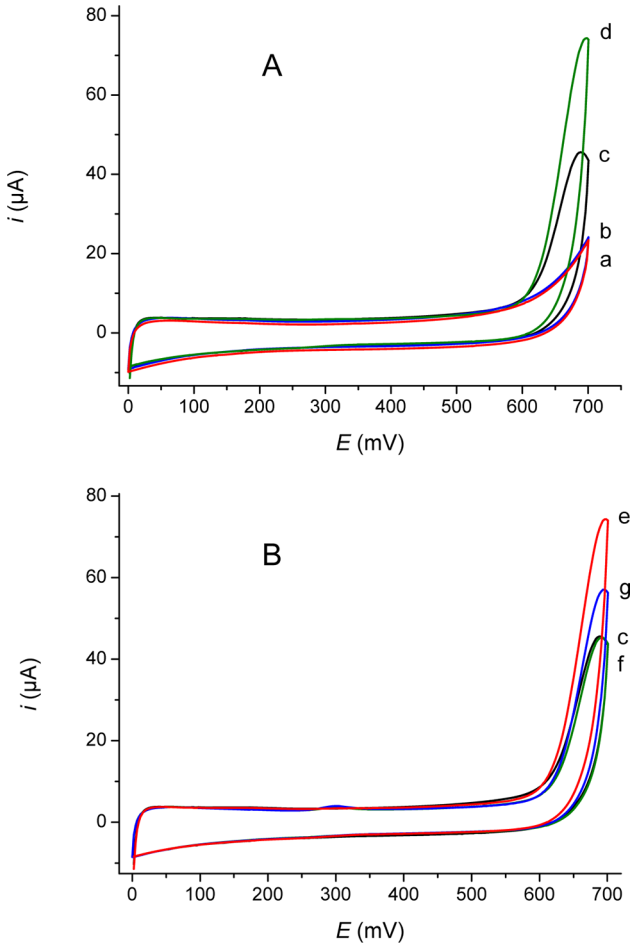

Figure 8. Cyclic voltammograms recorded in 0.1 M sodium phosphate buffer, pH 7.0, at a scan rate of 50 mV/s for: (A) XO-CD/*p*AuNP/SWNT/GCE and XO/*p*AuNP/SWNT/GCE without addition of xanthine (curves a and b, respectively) and after addition of 200 μM xanthine (curves d and c, respectively). (B) XO-CD/*p*AuNP/SWNT/GCE and XO/*p*AuNP/SWNT/GCE in the presence of 200 μM xanthine before (curves e and c, respectively) and after 1 h incubation in saturated 1-adamantane carboxylic acid solution (curves g and f, respectively).

7.0 saturated with 1-adamantane carboxylic acid. Since CDs form highly stable inclusion complexes with adamantane derivatives,[28] it was foreseen that the presence of saturated 1-adamantane carboxylic acid in the incubation medium could compete with the multiple host−guest interactions between the immobilized enzyme and the adamantane-coated Au nanoparticles electropolymerized network at the GCE surface. As a control, a *p*AuNP/SWNT/GCE modified with native XO was also checked under the same conditions.

Figure 8B shows as the peak current measured at +0.69 V did not significantly change for the XO/*p*AuNP/SWNT/GCE after 1 h incubation in the 1-adamantane carboxylic acid solution, suggesting that the activity of the native enzyme was not affected by the incubation process.[22,29] However, a noticeable decrease in the peak current was observed with the XO-CD/*p*AuNP/SWNT/GCE after incubation, suggesting lower amount of enzyme activity at the electrode surface. This effect could be caused by the competitive interaction of 1-adamantane carboxylic acid with the CD moieties attached to the enzyme surface, then affecting the supramolecular association of the enzyme with the adamantane moieties at the nanoparticles and

Table 1. Comparison of the Analytical Characteristics of the Developed Biosensors with Those Previously Reported for Other Electrochemical Xanthine Biosensors[a]

electrode	E (mV)	linear range (μM)	detection limit (μM)	sensitivity (mA/M)	K_M (μM)
XO/gelatin/graphite[34]	−50[b]	4.5−40	4.5	210	30
XO/PB/PPy/Au-NPs/Au[40]	−100[c]	1.0−20		0.19	43.2
XO/pTTCA/Au[37]	−350[b]	0.5−100	0.09	5.35	
XO-CMC-CD/ADA-Au[29]	+700[b]	300−10 400	200	0.25	9900
XO-ADA/pCD/Au[22]	+700[b]	310−6800	150	0.40	2100
XO/MWNT/GCE[38]	−400[c]	0.1−6	0.08		
SG/XO/MWNT/GCE[38]	−400[c]	0.2−10	0.1		
XO/laponite/GCE[31]	+390[c]	0.039−21	0.01	6.54	64
XO/$CaCO_3$−NPs/GCE[33]	+550[c]	2−250	2.0	11.9	
XO/HRP/$CaCO_3$−NPs/GCE[33]	−50[c]	0.4−50	0.1	2.8	127
XO/DWNT/CPE[30]	+900[b]	2.0−50		44.1	
XO/Pd−Pt/graphite[35]	−50[b]	1.5−70	1.5	390	58.5
XO/ZnO-NPs/PPy/Pt[41]	+380[b]	0.8−40	0.8		13.5
XO/c-MWNT/PANI/Pt[42]	+400[b]	0.6−58	0.6		
XO/Fe_3O_4@APTES-PEG/SWNT/SPE[36]	+600[b]	0.25−3.5	0.06	394	12.8
XO/Au-NPs/PVF/Pt[32]	+400[c]	2.5−560	0.75	0.91	393
XO/Pt-NPs/PVF/Pt[32]	+400[c]	2.0−660	0.6	1.67	286
XO/ox-graphite[39]	+600[b]	0.1−0.7	0.1		0.4
XO/ZnO-NPs/CHIT/c-SWNT/PANI/Pt[43]	+500[b]	0.1−100	0.1		
XO-CD/pAuNP/SWNT/GCE (present work)	+650[b]	0.05−9.5	0.04	178	3.2
Naf/XO-CD/pAuNP/SWNT/GCE (present work)	+650[b]	0.05 −9.5	0.04	152	3.8

[a]PB, Prussian Blue; PPy, polypyrrol; NPs, nanoparticles; pTTCA, poly-5, 2′:5′,2″-terthiophine-3-carboxylic acid; CMC-CD, cyclodextrin-branched carboxymethylcellulose; pCD, polymerized CD; MWNT, multiwalled carbon nanotubes; CGE, glassy carbon electrode; SG, silica sol−gel; DWNT, double-walled carbon nanotubes; CPE, carbon paste electrode; c-MWNT, carboxylated MWNT; PANI, polyaniline; APTES, (3-aminopropyl)-triethoxysilane; PEG, monomethoxypolyethylene glycol; SPE, gold screen-printed electrode; PVF, polyvinylferrocene; ox-Graphite, oxidized graphite; CHI, chitosan. [b]Ag/AgCl. [c]Saturated calomel electrode.

releasing certain amount of enzyme molecules from the electrode surface. However, further studies should be performed to demonstrate this hypothesis.

Nevertheless, it should be stated that there are other forces that should also contribute to the immobilization of XO-CD on the surface of pAuNP/SWNT/GCE besides the commented host−guest supramolecular interactions. The occurrence of physical adsorption of the enzyme derivative on the exposed SWNT-coated surface as well as electrostatic interactions with the charged groups at the surface of the nanoparticle-based matrix can play also a role in the overall enzyme immobilization process.

3.2. Analytical Performance of the Nanostructured Enzyme Electrode. The bioelectrode prepared through the supramolecular approach was used to construct an amperometric enzyme biosensor toward xanthine. The values to be selected for the working pH and applied potential were determined by checking the steady-state current and the signal-to- noise ratio measured for 500 nM xanthine. According to the obtained results (not shown), pH 7.0 and a detection potential value of +650 mV vs Ag/AgCl were selected for further work. It is well-known that the use of such a relatively high working potential would yield remarkable interferences from other electrochemically oxidizable substances such as ascorbic and uric acids. To minimize such adverse effects, the use of a Nafion thin film on the electrode surface was also evaluated[12] which would also serve to test the behavior of this well-known strategy with complex nanostructured biointerfaces such as the one developed in this work. Accordingly, the analytical characteristics of both enzyme electrode architectures prepared without (XO-CD/pAuNP/SWNT/GCE) and with Nafion coating (Naf/XO-CD/pAuNP/SWNT/GCE) were evaluated.

The XO-CD/pAuNP/SWNT/GCE enzyme electrode showed a fast and sensitive response to successive additions of xanthine, reaching 95% of the steady-state current in 5 s. Regarding the Naf/XO-CD/pAuNP/SWNT/GCE, a similar behavior was observed although the time of response was increased to about 9 s (data not shown). Both the XO-CD/pAuNP/SWNT/GCE and Naf/XO-CD/pAuNP/SWNT/GCE biosensors exhibited a linear dynamic range between 50 nM and 9.5 μM fitting to the following equations:

$$i\ (\mathrm{mA}) = 178c(\mathrm{xanthine/M}) + 3 \times 10^{-5}(\mathrm{XO\text{-}CD}/p\mathrm{AuNP/SWNT/GCE})$$

$$i\ (\mathrm{mA}) = 152c(\mathrm{xanthine/M}) + 2 \times 10^{-5}(\mathrm{Naf/XO\text{-}CD}/p\mathrm{AuNP/SWNT/GCE})$$

with correlation coefficients of 0.999 and 0.997 (n = 10) and sensitivities of 2.47 A/(M cm^2) and 2.12 A/(M cm^2) for the XO-CD/pAuNP/SWNT/GCE and Naf/XO-CD/pAuNP/SWNT/GCE biosensors, respectively. It is important to point out that coating of the bioelectrode surface with the Nafion film did not produce an important decrease in sensitivity. Moreover, as it can be deduced from data compiled in Table 1, the sensitivity of these biosensors ranks among the highest reported for other amperometric xanthine biosensors.

The detection limit achieved with both biosensors was calculated to be 40 nM, according to the 3SD/m criterion where m is the slope of the linear calibration graph and SD is the standard deviation for 10 different 50 nM xanthine amperometric measurements. As can be deduced from data in Table 1, this value is lower than most of those reported for other xanthine biosensor designs providing detection limits in

the nanomolar level, such as those using poly-5,2′:5′,2″-terthiophine-3-carboxylic acid modified Au electrodes,[37] multiwalled carbon nanotubes coated GCE,[38] and oxidized graphite,[39] although slightly higher than that reported for laponite-coated GCE.[31]

The apparent K_M values were estimated to be 3.2 μM and 3.8 μM for the XO-CD/*p*AuNP/SWNT/GCE and Naf/XO-CD/*p*AuNP/SWNT/GCE biosensors, respectively. It should be highlighted that these apparent K_M values were lower than those reported for the XO biosensors summarized in Table 1.

As mentioned above, coating with Nafion only reduced the sensitivity of the bioelectrode in about 14% while the detection limit, the K_M value and the range of linearity are similar to that of the uncoated electrode, suggesting that coating with Nafion did not significantly affect the electroanalytical performance of the biosensor.

It should be noted that the control bioelectrode (XO/*p*AuNP/SWNT/GCE) exhibited a poorer analytical performance: shorter linear range (1.3−9.5 μM), higher detection limit (1.0 μM) and lower sensitivity (1.2 A/M cm^2), than that achieved with the biosensors prepared with the CD-modified enzyme. Again these results suggested that native enzyme was poorly loaded on the nanostructured electrode in comparison with the modified enzyme, and that the formation of host−guest supramolecular association was involved in the immobilization of the XO-CD derivative. Comparing the sensitivity of this control bioelectrode with that obtained with XO-CD/pAuNP/SWNT/GCE, it could be deduced that the contribution of the host−guest supramolecular associations represented about 51% of the overall interactions involved in the immobilization process, assuming that glycosylation of XO with CD moieties did not affect the other contributing interaction forces.

The repeatability of the measurements carried out with one single XO-CD/*p*AuNP/SWNT/GCE or Naf/XO-CD/*p*AuNP/SWNT/GCE biosensor was checked for 500 nM xanthine (n = 10), yielding relative standard deviation (RSD) values of 3.9 and 5.2%, respectively. Moreover, the electrode-to-electrode reproducibility was calculated from the responses of ten different bioelectrodes prepared in the same manner toward 500 nM xanthine. The obtained RSD values were 6.7 and 8.6% for the XO-CD/*p*AuNP/SWNT/GCE and Naf/XO-CD/*p*AuNP/SWNT/GCE biosensors, respectively. The slightly higher RSD values observed for the Naf/XO-CD/*p*AuNP/SWNT/GCE should be related to the additional step of Nafion thin film formation during the preparation of the enzyme electrodes.

The selectivity of the biosensors was evaluated in the presence of eight possible interfering substances: glucose, sacarose, ethanol, acetic acid, lactic acid, citric acid, uric acid, and ascorbic acid. Figure 9 shows the influence of these possible interfering compounds added at a 5.0 μM concentration level on the amperometric signal measured for 500 nM xanthine. As can be observed, the XO-CD/*p*AuNP/SWNT/GCE biosensor showed excellent selectivity toward glucose, sacarose, ethanol, acetic acid, lactic acid and citric acid, yielding unaffected amperometric signals upon addition of these substances. However, as expected, a significant increase in the steady-state current was produced at the XO-CD/*p*AuNP/SWNT/GCE biosensor after addition of a 10-fold higher concentration of uric or ascorbic acid, showing the strong interference of these substances on the amperometric measurement for xanthine at the detection potential applied. Nevertheless, the extent of these interferences was dramatically decreased when the Naf/XO-CD/*p*AuNP/SWNT/GCE was employed, as expected considering the electrostatic repulsion between the negative charged Nafion thin film and the uricate and ascorbate anions at the working pH.[12]

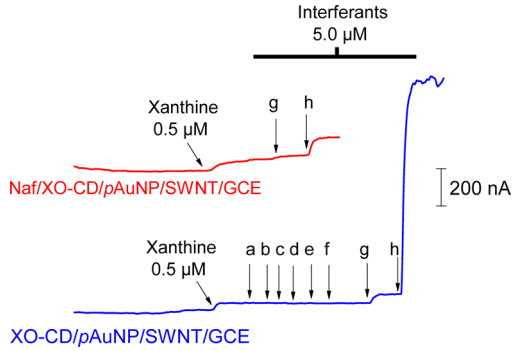

Figure 9. Amperometric responses of the XO-CD/*p*AuNP/SWNT/GCE and Naf/XO-CD/*p*AuNP/SWNT/GCE biosensors toward 500 nM xanthine upon addition of (a) glucose, (b) sacarose, (c) ethanol, (d) acetic acid, (e) lactic acid, (f) citric acid, (g) uric acid, and (h) ascorbic acid at a 5.0 μM concentration level.

The long-term stability of the XO-CD/*p*AuNP/SWNT/GCE and Naf/XO-CD/*p*AuNP/SWNT/GCE biosensors was evaluated by storing them at 4 °C under dry conditions and periodical evaluation of their analytical response toward 500 nM xanthine (see the Supporting Information). The XO-CD/*p*AuNP/SWNT/GCE biosensor retained high electroanalytical activity during the first week. After that, the response was progressively lost with time of storage according to a first-order kinetics progress, showing about 65 and 54% of its initial activity after 30 and 40 days of storage, respectively. The stability showed by this biosensor could be associated with the multivalence supramolecular strategy employed to immobilize the enzyme on the electrode surface.[18,29] In addition, it has been largely demonstrated that the stability of enzymes can be significantly improved by chemical glycosylation with CD derivatives.[18]

Interestingly, coating of the electrode with Nafion thin film improved largely the biosensor stability keeping about 91% of its electroanalytical activity after 40 days of storage. This fact suggested that the Nafion film presumably avoided the release of enzyme molecules from the electrode surface and preserved their three-dimensional active structure during storage. Similar results were previously described for other enzyme electrodes coated with Nafion thin films.[12]

CONCLUSIONS

The electropolymerization of polyfunctionalized Au nanoparticles bearing aniline, sulfonic acid, and adamantane residues through the formation of bis-aniline linkages on SWNTs-modified GCEs served as efficient electrode platforms to form supramolecular host−guest complexes with CD-modified enzymes. These electrode surfaces, exhibiting molecular receptor capacity, were in particular employed as support for the supramolecular immobilization of the glycoenzyme XO-ADA and further construction of an amperometric biosensor for xanthine. The enzyme electrode exhibited good sentitivity and stability, a very low detection limit, as well as fast electroanalytical response toward the analyte. In fact, the analytical performance of the supramolecular enzyme immobilization based biosensor ranked among the best achieved when

compared with those previosly reported for other XO electrochemical biosensors. Therefore, according to these results, we can anticipate the use of this bisaniline-cross-linked nanostructured network of metal nanoparticles on SWNT-coated electrodes as an excellent strategy to prepare enzyme biosensors with supramolecular architecture.

■ ASSOCIATED CONTENT

Supporting Information

Additional characterization of the nanoparticles and chronoamperometric and stability studies for the biosensors. This material is available free of charge via the Internet at http://pubs.acs.org.

■ AUTHOR INFORMATION

Corresponding Author

*Phone: +34 91 3944315. Fax: +34 91 3944329. E-mail: pingarro@quim.ucm.es (J.M.P.); rvillalonga@quim.ucm.es (R.V.).

Notes

The authors declare no competing financial interest.

■ ACKNOWLEDGMENTS

R. Villalonga acknowledge to Ramón & Cajal contract from the Spanish Ministry of Science and Innovation. Financial support from the Spanish Ministry of Science and Innovation CTQ2011-24355, CTQ2009-12650, CTQ2009-09351, and Comunidad de Madrid S2009/PPQ-1642, programme AVANSENS is gratefully acknowledged.

■ REFERENCES

(1) Grieshaber, D.; MacKenzie, R.; Vörös, J.; Reimhult, E. *Sensors* **2008**, *8*, 1400−1458.
(2) Wang, J. *Analyst* **2005**, *130*, 421−426.
(3) Kumar, C. S. S. R. *Nanomaterials for Biosensors. Nanotechnologies for the Life Sciences*; Wiley-VCH:, Weinheim, Germany, 2006, Vol. *8*.
(4) Li, S.; Singh, J.; Li, H.; Banerjee, I. A. *Biosensor Nanomaterials*; Wiley-VCH: Weinheim, Germany, 2011.
(5) Shao, Y.; Wang, J.; Wu, H.; Liu, J.; Aksay, I. A.; Lin, Y. *Electroanalysis* **2010**, *22*, 1027−1036.
(6) Yang, W.; Ratinac, K. R.; Ringer, S. P.; Thordarson, P.; Gooding, J. J.; Braet, F. *Angew. Chem., Int. Ed.* **2010**, *49*, 2114−2138.
(7) Yeom, S. H.; Kang, B. H.; Kim, K. J.; Kang, S. W. *Front. Biosci.* **2011**, *16*, 997−1023.
(8) Pingarrón, J. M.; Yáñez-Sedeño, P.; González-Cortés, A. *Electrochim. Acta* **2008**, *53*, 5848−5866.
(9) Luo, X.; Morrin, A.; Killard, A. J.; Smyth, M. R. *Electroanalysis* **2006**, *18*, 319−326.
(10) Agüi, L.; Yañez-Sedeño, P.; Pingarrón, J. M. *Anal. Chim. Acta* **2008**, *622*, 11−47.
(11) Wang, J. *Electroanalysis* **2005**, *17*, 7−14.
(12) Eguílaz, M.; Villalonga, R.; Agüí, L.; Yáñez-Sedeño, P.; Pingarrón, J. M. *J. Electroanal. Chem.* **2011**, *661*, 171−178.
(13) Riskin, M.; Tel-Vered, R.; Willner, I. *Adv. Mater.* **2010**, *22*, 1387−1391.
(14) Frasconi, M.; Tel-Vered, R.; Riskin, M.; Willner, I. *Anal. Chem.* **2010**, *82*, 2512−2519.
(15) Villalonga, R.; Díez, P.; Yañez-Sedeño, P.; Pingarrón, J. M. *Electrochim. Acta* **2011**, *56*, 4672−4677.
(16) Villalonga, R.; Diez, P.; Casado, S.; Eguílaz, M.; Yañez-Sedeño, P.; Pingarrón, J. M. *Analyst* **2012**, *137*, 342−348.
(17) Fragoso, A.; Caballero, J.; Almirall, E.; Villalonga, R.; Cao, R. *Langmuir* **2002**, *18*, 5051−5054.
(18) Villalonga, R.; Cao, R.; Fragoso, A. *Chem. Rev.* **2007**, *107*, 3088−3116.
(19) Villalonga, R.; Cao, R.; Fragoso, A.; Damiao, A. E.; Ortiz, P. D.; Caballero, J. *J. Mol. Catal. B: Enzym.* **2005**, *35*, 79−85.
(20) Camacho, C.; Chico, B.; Cao, R.; Matías, J. C.; Hernández, J.; Palchetti, I.; Simpson, B. K.; Mascini, M.; Villalonga, R. *Biosens. Bioelectron.* **2009**, *24*, 2028−2033.
(21) Camacho, C.; Matías, J. C.; Cao, R.; Matos, M.; Chico, B.; Hernández, J.; Longo, M. A.; Sanromán, M. A.; Villalonga, R. *Langmuir* **2008**, *24*, 7654−7657.
(22) Villalonga, R.; Camacho, C.; Cao, R.; Hernández, J.; Matias, J. C. *Chem. Commun.* **2007**, 942−944.
(23) Baussanne, I.; Benito, J. M.; Ortiz Mellet, C.; García Fernández, J. M.; Lawa, H.; Defaye, J. *Chem. Commun.* **2000**, 1489−1490.
(24) Fernández, M.; Fragoso, A.; Cao, R.; Villalonga, R. *J. Mol. Catal. B: Enzym.* **2003**, *21*, 133−141.
(25) Tlili, A.; Abdelghani, A.; Hleli, S.; Maaref, M. A. *Sensors* **2004**, *4*, 105−114.
(26) Lu, T. L.; Tsai, Y. C. *Sens. Actuators, B* **2010**, *148*, 590−594.
(27) Duić, L.; Mandić, Z.; Kovač, S. *Electrochim. Acta* **1995**, *40*, 1681−1688.
(28) Cromwell, W. C.; Byström, K.; Eftink, M. R. *J. Phys. Chem.* **1985**, *89*, 326−332.
(29) Villalonga, R.; Matos, M.; Cao, R. *Electrochem. Commun.* **2007**, *9*, 454−458.
(30) Anik, Ü.; Çevi, S. *Microchim. Acta* **2009**, *166*, 209−213.
(31) Shan, D.; Wang, Y. N.; Xue, H. G.; Cosnier, S.; Ding, S. N. *Biosens. Bioelectron.* **2009**, *24*, 3556−3561.
(32) Bas, S. Z.; Gulce, H.; Yildiz, S.; Gulce, A. *Talanta* **2011**, *87*, 189−196.
(33) Shan, D.; Wang, Y.; Xue, H.; Cosnier, S. *Sens. Actuators, B* **2009**, *136*, 510−515.
(34) Dimcheva, N.; Horozova, E.; Jordanova, Z. *Z. Naturforsch., C* **2002**, *57*, 883−889.
(35) Dodevska, T.; Horozova, E.; Dimcheva, N. *Cent. Eur. J. Chem.* **2010**, *8*, 19−27.
(36) Villalonga, R.; Villalonga, M. L.; Díez, P; Pingarrón, J. M. *J. Mater. Chem.* **2011**, *21*, 12858−12864.
(37) Rahman, M. A.; Won, M. S.; Shim, Y. B. *Electroanalysis* **2007**, *19*, 631−637.
(38) Gao, Y.; Shen, C.; Di, J.; Tu, Y. *Mater. Sci. Eng., C* **2009**, *29*, 2213−2216.
(39) Devi, R.; Narang, J.; Yadav, S.; Pundir, C. S. *J. Anal. Chem.* **2012**, *67*, 273−277.
(40) Liu, Y.; Nie, L.; Tao, W.; Yao, S. *Electroanalysis* **2004**, *16*, 1271−1278.
(41) Devi, R.; Thakur, M.; Pundir, C. S. *Biosens. Bioelectron.* **2011**, *26*, 3420−3426.
(42) Devi, R.; Yadav, S.; Pundir, C. S. *Biochem. Eng. J.* **2011**, *58*−*59*, 148−153.
(43) Devi, R.; Yadav, S.; Pundir, C. S. *Analyst* **2012**, *137*, 754−759.